Seismic inverse problem using multi-components data with Full Reciprocity-gap Waveform Inversion

Florian Faucher

Seismic inverse problem using multi-components data with Full Reciprocity-gap Waveform Inversion

Florian Faucher[1],

Giovanni Alessandrini[2], Hélène Barucq[1], Maarten V. de Hoop[3], Romina Gaburro[4] and Eva Sincich[2].

ICIAM 2019, Valencia, Spain

July 19th, 2019

[1] Project-Team Magique-3D, Inria Bordeaux Sud-Ouest, France.

[2] Dipartimento di Matematica e Geoscienze, Università di Trieste, Italy.

[3] Department of Computational and Applied Mathematics and Earth Science, Rice University, Houston, USA

[4] Department of Mathematics and Statistics, Health Research Institute (HRI), University of Limerick, Ireland.

Overview

1. Introduction
2. Time-Harmonic Inverse Problem, FWI
   - Dual-sensors data
   - Iterative reconstruction algorithm
3. Reconstruction procedure using dual-sensors data
4. Numerical experiments
   - Experiments for acoustic media
   - Comparison of misfit functions
   - Changing the numerical acquisition with $\mathcal{J}_{\mathcal{G}}$
   - Extension toward elasticity
5. Conclusion

Plan

Seismic exploration inverse problem

Reconstruction of subsurface Earth properties from seismic campaign: collection of **wave** propagation data at the surface.

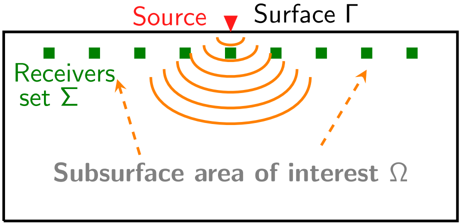

- Reflection (back-scattered) partial data,
- **nonlinear, ill-posed inverse problem.**

Seismic exploration inverse problem

Reconstruction of subsurface Earth properties from seismic campaign: collection of **wave** propagation data at the surface.

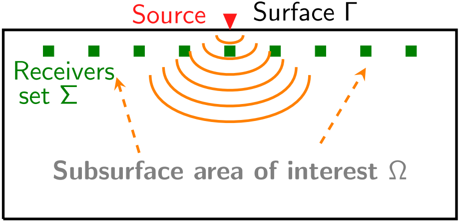

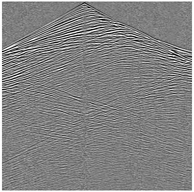

- Reflection (back-scattered) partial data,
- **nonlinear, ill-posed inverse problem.**

Plan

2. Time-Harmonic Inverse Problem, FWI
   - Dual-sensors data
   - Iterative reconstruction algorithm

Time-harmonic wave equation

We consider propagation in acoustic media, given by the Euler's equations, heterogeneous medium parameters κ and ρ:

$$\begin{cases} -\mathrm{i}\omega\rho(\boldsymbol{x})\boldsymbol{v}(\boldsymbol{x}) = -\nabla p(\boldsymbol{x}), \\ -\mathrm{i}\omega p(\boldsymbol{x}) = -\kappa(\boldsymbol{x})\nabla\cdot\boldsymbol{v}(\boldsymbol{x}) + f(\boldsymbol{x}). \end{cases}$$

p: scalar pressure field,

$\boldsymbol{v}$: vectorial velocity field,

f: source term,

κ: bulk modulus,

ρ: density,

ω: angular frequency.

Time-harmonic wave equation

We consider propagation in acoustic media, given by the Euler's equations, heterogeneous medium parameters κ and ρ:

$$\begin{cases} -\mathrm{i}\omega\rho(\boldsymbol{x})\boldsymbol{v}(\boldsymbol{x}) = -\nabla p(\boldsymbol{x}), \\ -\mathrm{i}\omega p(\boldsymbol{x}) = -\kappa(\boldsymbol{x})\nabla\cdot\boldsymbol{v}(\boldsymbol{x}) + f(\boldsymbol{x}). \end{cases}$$

- p: scalar pressure field,
- $\boldsymbol{v}$: vectorial velocity field,
- f: source term,
- κ: bulk modulus,
- ρ: density,
- ω: angular frequency.

The system reduces to the Helmholtz equation when ρ is constant,

$$(-\omega^2 c(\boldsymbol{x})^{-2} - \Delta)p(\boldsymbol{x}) = 0,$$

$$\text{with} \quad c(\boldsymbol{x}) = \sqrt{\kappa(\boldsymbol{x})\rho(\boldsymbol{x})^{-1}}.$$

Measurements from dual-sensors

The quantitative inverse problem aims the recovery of the physical parameters from **surface field measurements**.

Dual-sensors record the pressure and vertical velocity:

$$\mathcal{F}(m = (\kappa,\, \rho)) = \left\{ p(\boldsymbol{x}_1),\, p(\boldsymbol{x}_2), \ldots,\, p(\boldsymbol{x}_{n_{rcv}}) \right\}; \quad \left\{ v_n(\boldsymbol{x}_1),\, v_n(\boldsymbol{x}_2), \ldots,\, v_n(\boldsymbol{x}_{n_{rcv}}) \right\}.$$

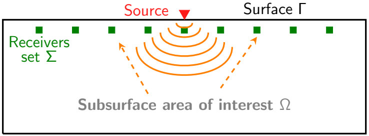

D. Carlson, N. D. Whitmore *et al.*
Increased resolution of seismic data from a dual-sensor streamer cable – Imaging of primaries and multiples using a dual-sensor towed streamer
SEG, 2007 – 2010

CGG & Lundun Norway (2017 – 2018)
TopSeis acquisition (`www.cgg.com/en/What-We-Do/Offshore/Products-and-Solutions/TopSeis`)

Full Waveform Inversion (FWI)

FWI provides a **quantitative reconstruction** of the subsurface parameters by solving a minimization problem,

$$\min_{m \in \mathcal{M}} \quad \mathcal{J}(m) = \frac{1}{2} \|\mathcal{F}(m) - d\|^2.$$

- d are the observed data,
- $\mathcal{F}(m)$ represents the simulation using an initial model m:

P. Lailly
The seismic inverse problem as a sequence of before stack migrations
Conference on Inverse Scattering: Theory and Application, SIAM, 1983

A. Tarantola
Inversion of seismic reflection data in the acoustic approximation
Geophysics, 1984

A. Tarantola
Inversion of travel times and seismic waveforms
Seismic tomography, 1987

FWI, iterative minimization

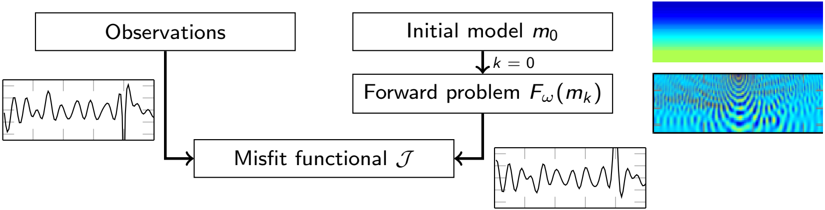

FWI, iterative minimization

Observations

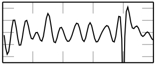

Initial model m_0

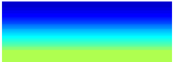

$k = 0$

Forward problem $F_\omega(m_k)$

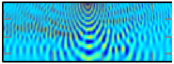

Misfit functional $\mathcal{J}$

Optimization procedure

1. Gradient
2. Search direction s_k
3. Line search α_k

$k = k + 1$

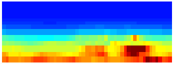

update model
$m_{k+1} = m_k + \alpha_k s_k$

Update ω

FWI, iterative minimization

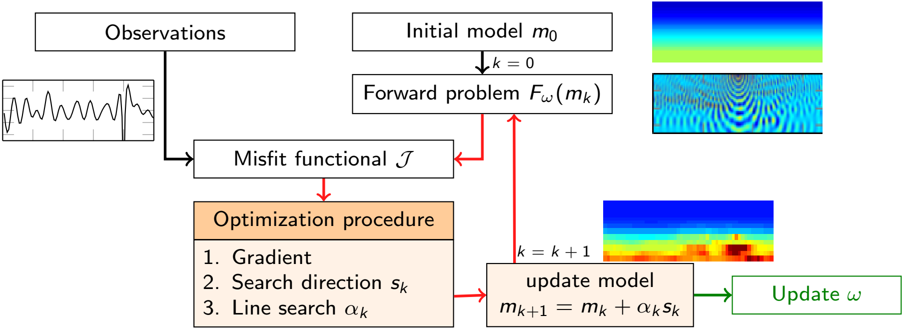

Numerical methods

- Adjoint-method for the gradient computation, L-BFGS method,
- **Hybridizable Discontinuous Galerkin** discretization method,
- elasticity, anisotropy, viscosity.

Hybridizable Discontinuous Galerkin discretization

Hybridizable Discontinuous Galerkin (HDG) discretization:

- **global matrix** with the **faces d.o.f.** only,
- **local problem** to have the volume solution on DG d.o.f.

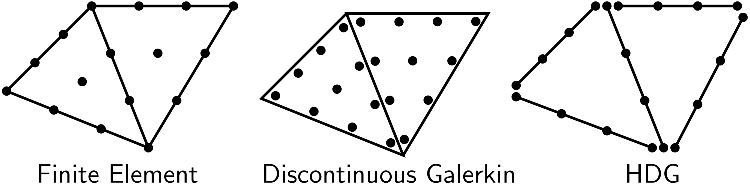

- Global matrix needs less memory than FE and DG (order),
- the local problems are small and embarrassingly parallel,
- 1st order: same accuracy for p and $\boldsymbol{v}$,
- topography, sub-surface shapes.

Plan

3. Reconstruction procedure using dual-sensors data

Iterative reconstruction with dual-sensors data

- Compare the pressure and velocity fields separately ($L2$):

$$\mathcal{J}_{L2} = \sum_{source} \frac{1}{2}\|\mathcal{F}_p^{(s)} - d_p^{(s)}\|^2 + \frac{1}{2}\|\mathcal{F}_v^{(s)} - d_v^{(s)}\|^2.$$

Iterative reconstruction with dual-sensors data

- Compare the pressure and velocity fields separately ($L2$):

$$\mathcal{J}_{L2} = \sum_{source} \frac{1}{2} \| \mathcal{F}_p^{(s)} - d_p^{(s)} \|^2 + \frac{1}{2} \| \mathcal{F}_v^{(s)} - d_v^{(s)} \|^2.$$

- Compare the reciprocity-gap:

$$\mathcal{J}_{\mathcal{G}} = \frac{1}{2} \sum_{s_1} \sum_{s_2} \| d_v^{(s_1)\,T} \mathcal{F}_p^{(s_2)} - d_p^{(s_1)\,T} \mathcal{F}_v^{(s_2)} \|^2.$$

G. Alessandrini, M.V. de Hoop, F. F., R. Gaburro and E. Sincich
Inverse problem for the Helmholtz equation with Cauchy data: reconstruction with conditional well-posedness driven iterative regularization
ESAIM: M2AN, 2019.

Reciprocity-gap waveform inversion

$$\mathcal{J}_{\mathcal{G}} = \frac{1}{2} \sum_{s_1} \sum_{s_2} \| d_v^{(s_1)\,T} \mathcal{F}_p^{(s_2)} - d_p^{(s_1)\,T} \mathcal{F}_v^{(s_2)} \|^2.$$

- Motivated by Green's identity (using variational formulation).

Reciprocity-gap waveform inversion

$$\mathcal{J}_{\mathcal{G}} = \frac{1}{2} \sum_{s_1} \sum_{s_2} \| d_v^{(s_1)\,T} \mathcal{F}_p^{(s_2)} - d_p^{(s_1)\,T} \mathcal{F}_v^{(s_2)} \|^2 .$$

- Motivated by Green's identity (using variational formulation).
- Reciprocity-gap functional from inverse scattering with Cauchy data.

R. Kohn and M. Vogelius
Determining conductivity by boundary measurements II. Interior results
Communications on Pure and Applied Mathematics, 1985.

D. Colton and H. Haddar
An application of the reciprocity gap functional to inverse scattering theory
Inverse Problems 21 (1), 2005, 383398.

G. Alessandrini, M.V. de Hoop, F. F., R. Gaburro and E. Sincich
Inverse problem for the Helmholtz equation with Cauchy data: reconstruction with conditional well-posedness driven iterative regularization
ESAIM: M2AN, 2019.

T. van Leeuwen and W. A. Mulder
A correlation-based misfit criterion for wave-equation traveltime tomography
Geophysical Journal International, 2010

Stability results

Lipschitz-type stability for the Helmholtz equation with partial data,

$$\|m_1 - m_2\| \leq \mathcal{C}\big(\mathcal{J}_{\mathcal{G}}(m_1, m_2)\big)^{1/2},$$

Stability results

Lipschitz-type stability for the Helmholtz equation with partial data,

$$\|m_1 - m_2\| \leq \mathcal{C}\left(\mathcal{J}_{\mathcal{G}}(m_1, m_2)\right)^{1/2},$$

- for piecewise linear parameters.
- Using back-scattered data from one side in a domain with free surface and absorbing conditions,

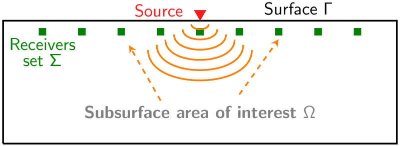

G. Alessandrini, M.V. de Hoop, R. Gaburro and E. Sincich
Lipschitz stability for a piecewise linear Schrödinger potential from local Cauchy data
arXiv:1702.04222, 2017.

G. Alessandrini, M.V. de Hoop, F. F., R. Gaburro and E. Sincich
Inverse problem for the Helmholtz equation with Cauchy data: reconstruction with conditional well-posedness driven iterative regularization
ESAIM: M2AN, 2019.

Main feature

It allows the separation of numerical and observational sources:

$$\mathcal{J}_{\mathcal{G}} = \frac{1}{2} \sum_{s_1} \sum_{s_2} \| d_v^{(s_1)\,T} \mathcal{F}_p^{(s_2)} - d_p^{(s_1)\,T} \mathcal{F}_v^{(s_2)} \|^2.$$

Main feature

It allows the separation of numerical and observational sources:

$$\mathcal{J}_{\mathcal{G}} = \frac{1}{2} \sum_{s_1} \sum_{s_2} \| d_v^{(s_1)\,T} \mathcal{F}_p^{(s_2)} - d_p^{(s_1)\,T} \mathcal{F}_v^{(s_2)} \|^2.$$

- s_1 is fixed by the observational setup,
- s_2 is chosen for the numerical comparisons,

- arbitrary positions of computational source,
- no need for a priori information on the observational source: position and wavelet are not required,
- not possible with the traditional misfit.

Plan

4. Numerical experiments
   - Experiments for acoustic media
   - Comparison of misfit functions
   - Changing the numerical acquisition with $\mathcal{J}_{\mathcal{G}}$
   - Extension toward elasticity

Experiment setup

3D velocity model 2.5 × 1.5 × 1.2km using dual-sensors data.

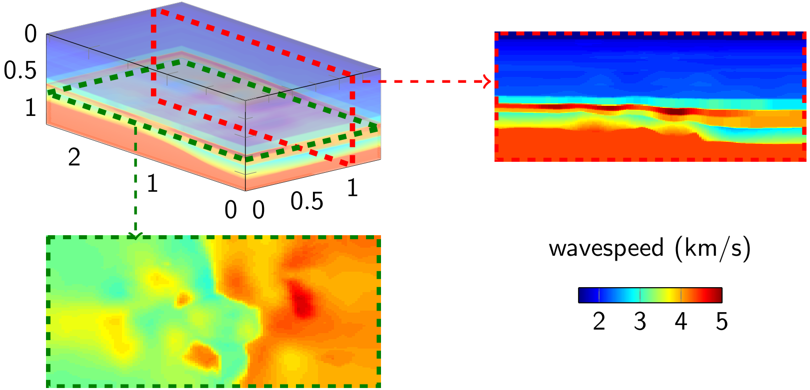

Experiment setup

We work with time-domain data acquisition.

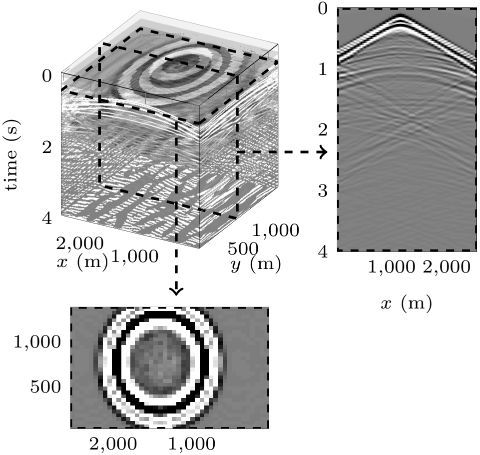

Experiment setup

We work with time-domain data (pressure and velocity).

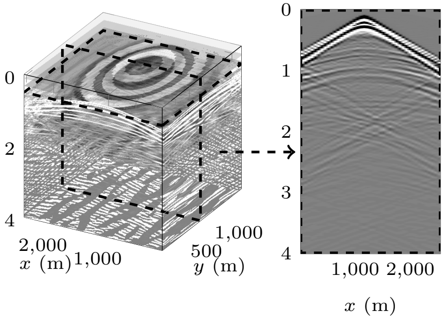

Acquisition for the measures

- 160 sources,
- 100 m depth,
- point source,

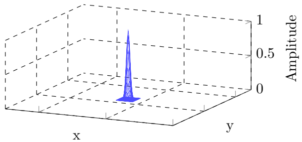

For the reconstruction, we apply a Fourier transform of the time data.

Comparison of misfit functional

We respect the observational acquisition setup and perform the minimization of $\mathcal{J}_{L2}$ or $\mathcal{J}_{\mathcal{G}}$, frequency from 3 to 15Hz.

$$\mathcal{J}_{L2} = \sum_{source} \frac{1}{2} \| \mathcal{F}_p^{(s)} - d_p^{(s)} \|^2 + \frac{1}{2} \| \mathcal{F}_v^{(s)} - d_v^{(s)} \|^2.$$

$$\mathcal{J}_{\mathcal{G}} = \frac{1}{2} \sum_{source} \sum_{source} \| d_v^{(s_1)\,T} \mathcal{F}_p^{(s_2)} - d_p^{(s_1)\,T} \mathcal{F}_v^{(s_2)} \|^2.$$

Comparison of misfit functional

We respect the observational acquisition setup and perform the minimization of $\mathcal{J}_{L2}$ or $\mathcal{J}_{\mathcal{G}}$, frequency from 3 to 15Hz.

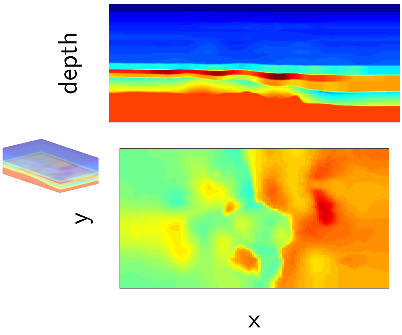

(a) True velocity

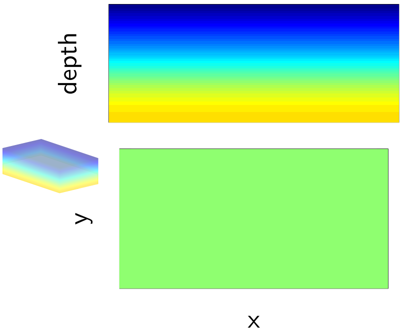

(b) Starting velocity

Comparison of misfit functional

We respect the observational acquisition setup and perform the minimization of $\mathcal{J}_{L2}$ or $\mathcal{J}_{\mathcal{G}}$, frequency from 3 to 15Hz.

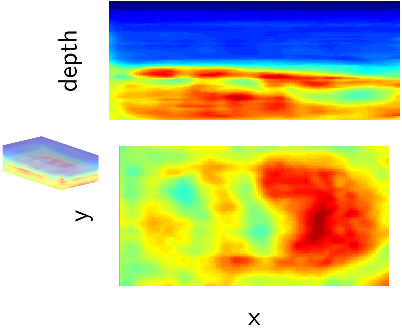

(a) Using $\mathcal{J}_{L2}$

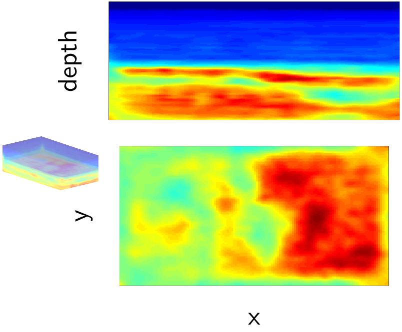

(b) Using $\mathcal{J}_{\mathcal{G}}$

Comparison of misfit functional

We respect the observational acquisition setup and perform the minimization of $\mathcal{J}_{L2}$ or $\mathcal{J}_{\mathcal{G}}$, frequency from 3 to 15Hz.

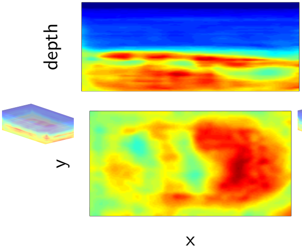

(a) Using $\mathcal{J}_{L2}$

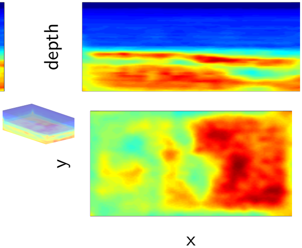

(b) Using $\mathcal{J}_{\mathcal{G}}$

But the major advantage of $\mathcal{J}_{\mathcal{G}}$ is the possibility to consider alternative acquisition setup.

Experiment with different obs. and sim. acquisition

$$\min \mathcal{J}_{\mathcal{G}} = \frac{1}{2} \sum_{s_1} \sum_{s_2} \| d_v^{(s_1)\,T} \mathcal{F}_p^{(s_2)} - d_p^{(s_1)\,T} \mathcal{F}_v^{(s_2)} \|^2 .$$

Acquisition for the measures s_1

- 160 sources,
- 100 m depth,
- point source,

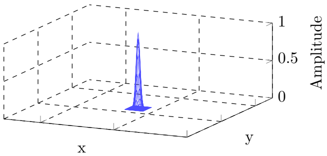

Experiment with different obs. and sim. acquisition

$$\min \mathcal{J}_{\mathcal{G}} = \frac{1}{2}\sum_{s_1}\sum_{s_2} \| d_v^{(s_1)\,T} \mathcal{F}_p^{(s_2)} - d_p^{(s_1)\,T} \mathcal{F}_v^{(s_2)} \|^2.$$

Acquisition for the measures s_1

- 160 sources,
- 100 m depth,
- point source,

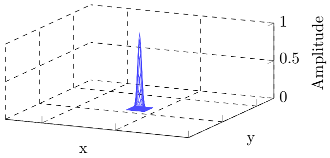

Arbitrary numerical acquisition s_2

- **5 sources**,
- **80**m **depth**,
- **multi-point sources**,

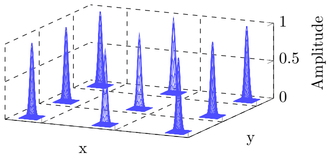

- No need to known observational source wavelet.
- Differentiation impossible with least squares types misfit.

Experiment with different obs. and sim. acquisition

Data from frequency between 3 to 15 Hz, domain size $2.5 \times 1.5 \times 1.2$ km,
Simulation using 5 sources only.

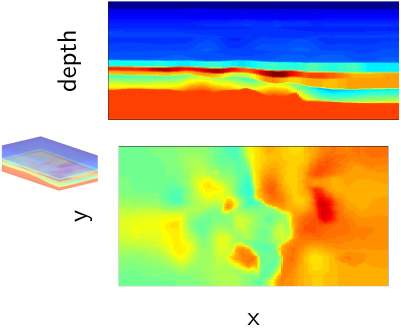

(a) True velocity

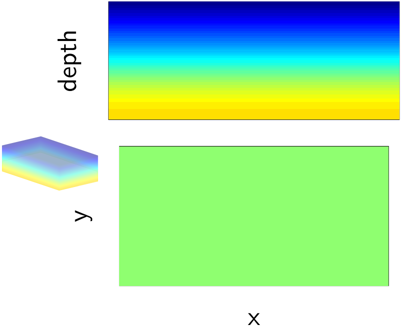

(b) Starting velocity

Experiment with different obs. and sim. acquisition

Frequency from 3 to 15 Hz, 2.5 $\times$ 1.5 $\times$ 1.2 km,
Simulation using 5 sources only. **-33%** computational time.

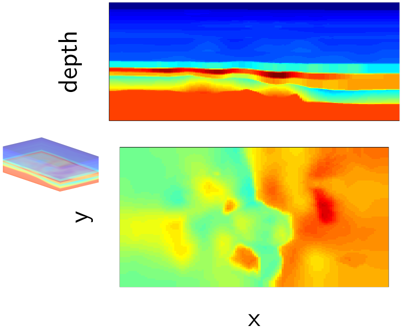

(a) True velocity

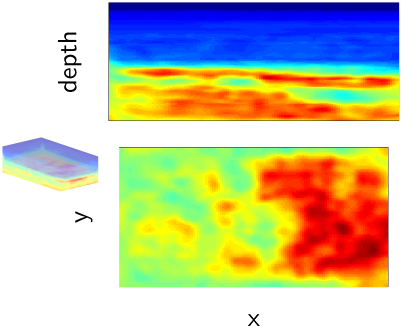

(b) 15 Hz reconstruction

Reciprocity-gap for elasticity

Reciprocity-gap for elasticity

Wave propagation in elastic media

$$-\nabla \cdot \underline{\sigma}(\boldsymbol{x}) - \omega^2 \rho(\boldsymbol{x}) \boldsymbol{u}(\boldsymbol{x}) = \boldsymbol{g}(\boldsymbol{x}),$$

σ is the stress tensor; elastic isotropy, Lamé parameters λ and μ:

$$\underline{\sigma} = \lambda \mathrm{Tr}(\underline{\epsilon}) I_d + 2\mu\underline{\epsilon}.$$

Reciprocity-gap for elasticity

Wave propagation in elastic media

$$-\nabla \cdot \underline{\sigma}(\boldsymbol{x}) - \omega^2 \rho(\boldsymbol{x}) \boldsymbol{u}(\boldsymbol{x}) = \boldsymbol{g}(\boldsymbol{x}),$$

σ is the stress tensor; elastic isotropy, Lamé parameters λ and μ:

$$\underline{\sigma} = \lambda \mathrm{Tr}(\underline{\epsilon}) I_d + 2\mu\underline{\epsilon}.$$

Three (heterogeneous) parameters to characterize the medium:

- λ and μ, or $c_p = \sqrt{(\lambda + 2\mu)/\rho}$, $c_s = \sqrt{\mu/\rho}$
- Density ρ.

Increased computational requirement and the ill-posedness of the inverse problem.

Elastic reciprocity formula

In elasticity, reciprocity needs measurements of σ and $\boldsymbol{u}$

$$\mathcal{F}(m := (\lambda, \mu, \rho)) = \left\{ \boldsymbol{u}(\boldsymbol{x}) \mid_{\Sigma},\ (\underline{\sigma}(\boldsymbol{x}) \cdot n) \mid_{\Sigma} \right\}.$$

Elastic reciprocity formula

In elasticity, reciprocity needs measurements of σ and $\boldsymbol{u}$

$$\mathcal{F}(m := (\lambda, \mu, \rho)) = \left\{ \boldsymbol{u}(\boldsymbol{x}) \mid_\Sigma,\ (\underline{\sigma}(\boldsymbol{x}) \cdot n) \mid_\Sigma \right\}.$$

$$\mathcal{J}_{\mathcal{G}} = \frac{1}{2} \sum_{s_1} \sum_{s_2} \| d_{\boldsymbol{u}}^{(s_1)\,T} \mathcal{F}_{\sigma \cdot n}^{(s_2)} - d_{\sigma \cdot n}^{(s_1)\,T} \mathcal{F}_{\boldsymbol{u}}^{(s_2)} \|^2.$$

Pluto model

2D elastic models of size 31 $\times$ 7km.

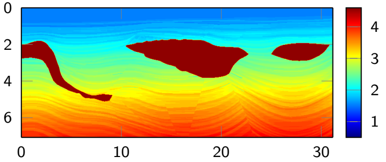

(a) P-wave speed

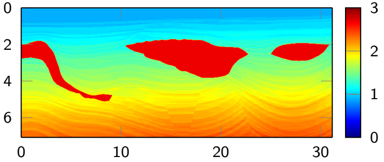

(b) S-wave speed

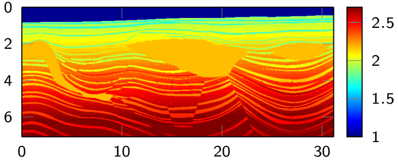

(c) Density

Pluto model

2D elastic models of size 31 × 7km.

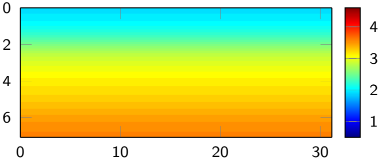

(a) P-wave speed

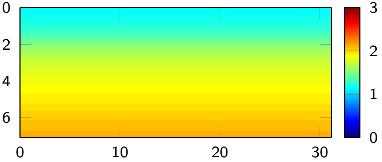

(b) S-wave speed

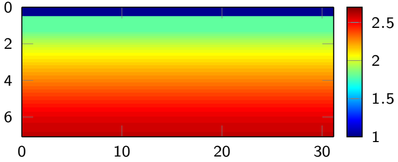

(c) Density

Reconstruction setup

- The density remains fixed; frequency from 0.50 to 7 Hz,
- Low frequency could be replaced by complex frequency (Laplace domain) or a priori information.

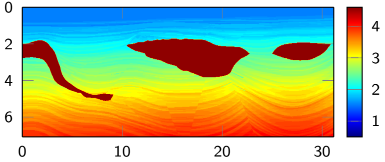

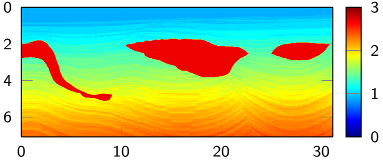

Observational acquisition:

- 150 sources,
- 20 m depth.

Computational acquisition:

- 30 sources,
- 10 m depth.

Reciprocity waveform inversion

- The density remains fixed; frequency from 0.50 to 7 Hz,
- Low frequency could be replaced by complex frequency (Laplace domain) or a priori information.

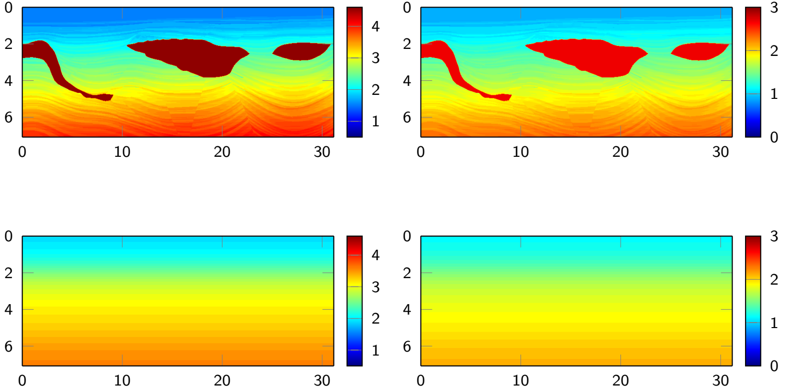

Reciprocity waveform inversion

- The density remains fixed; frequency from 0.50 to 7 Hz,
- Low frequency could be replaced by complex frequency (Laplace domain) or a priori information.

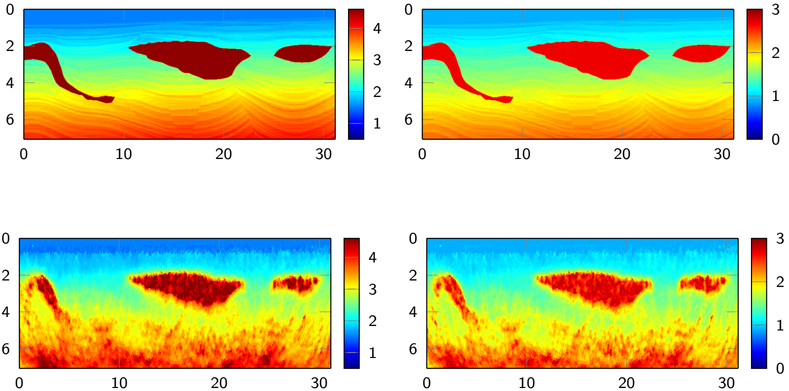

Plan

5 Conclusion

Conclusion

Quantitative time-harmonic inverse wave problem:

- Hybridizable Discontinuous Galerkin discretization, HPC,
- large scale optimization scheme using back-scattered data,
- acoustic, elastic, anisotropy, 2D, 3D, attenuation,
- stability and convergence analysis.

Reciprocity-gap waveform inversion:

- minimal information on the acquisition setup,
- reduced computational cost,
- other applications (elasticity, seismology, helioseismology),
- perspective: design efficient setup; data (rotational seismology).

Conclusion

Quantitative time-harmonic inverse wave problem:

- Hybridizable Discontinuous Galerkin discretization, HPC,
- large scale optimization scheme using back-scattered data,
- acoustic, elastic, anisotropy, 2D, 3D, attenuation,
- stability and convergence analysis.

Reciprocity-gap waveform inversion:

- minimal information on the acquisition setup,
- reduced computational cost,
- other applications (elasticity, seismology, helioseismology),
- perspective: design efficient setup; data (rotational seismology).

THANK YOU

Bibliography 1/2

D. Carlson, N. D. Whitmore *et al.*
Increased resolution of seismic data from a dual-sensor streamer cable – Imaging of primaries and multiples using a dual-sensor towed streamer
SEG, 2007 – 2010

CGG & Lundun Norway (2017 – 2018)
TopSeis acquisition (`www.cgg.com/en/What-We-Do/Offshore/Products-and-Solutions/TopSeis`)

P. Lailly
The seismic inverse problem as a sequence of before stack migrations
Conference on Inverse Scattering: Theory and Application, SIAM, 1983

A. Tarantola
Inversion of seismic reflection data in the acoustic approximation
Geophysics, 1984

A. Tarantola
Inversion of travel times and seismic waveforms
Seismic tomography, 1987

H. Barucq, H. Calandra, G. Chavent, F. Faucher
A priori estimates of attraction basins for velocity model reconstruction by time-harmonic Full Waveform Inversion and Data Space Reflectivity formulation
Research Report, 2019, `https://hal.archives-ouvertes.fr/hal-02016373/file/RR-9253.pdf` .

G. Alessandrini, S. Vessella
Lipschitz stability for the inverse conductivity problem
Adv. in Appl. Math., 2005

E. Beretta, M. V. de Hoop, F. Faucher, O. Scherzer
Inverse boundary value problem for the Helmholtz equation: quantitative conditional Lipschitz stability estimates
SIAM Journal on Mathematical Analysis, 2016

Bibliography 2/2

G. Alessandrini, M.V. de Hoop, F. F., R. Gaburro and E. Sincich
Inverse problem for the Helmholtz equation with Cauchy data: reconstruction with conditional well-posedness driven iterative regularization
ESAIM: M2AN, 2019.

R. Kohn and M. Vogelius
Determining conductivity by boundary measurements II. Interior results
Communications on Pure and Applied Mathematics, 1985.

D. Colton and H. Haddar
An application of the reciprocity gap functional to inverse scattering theory
Inverse Problems 21 (1), 2005, 383398.

G. Alessandrini, M.V. de Hoop, R. Gaburro and E. Sincich
Lipschitz stability for a piecewise linear Schrödinger potential from local Cauchy data
arXiv:1702.04222, 2017.

M. Grote, M. Kray, U. Nahum
Adaptive eigenspace method for inverse scattering problems in the frequency domain
Inverse Problems, 2017.

M. Grote, U. Nahum
Adaptive eigenspace for multi-parameter inverse scattering problems
Computers & Mathematics with Applications, 2019.

H. Barucq, F. Faucher, O. Scherzer
Eigenvector Model Descriptors for Solving an Inverse Problem of Helmholtz Equation
arXiv preprint arXiv:1903.08991 (2019).